

ORBITAL CHARACTERIZATION OF IGNEOUS AND AQUEOUS OUTCROPS IN THE TYRRHENA TERRA REGION OF MARS. J. L. Bishop¹, C. E. Viviano², M. D. Lane³, D. Tirsch⁴, D. Loizeau⁵, L. L. Tornabene⁶, and R. Jaumann^{4,7}, ¹SETI Institute (Mountain View, CA; jbishop@seti.org), ²Johns Hopkins University Applied Physics Lab (Laurel, MD), ³Fibernetics LLC (Lititz, PA), ⁴German Aerospace Center (DLR, Berlin, Germany), ⁵University of Western Ontario (London, Canada), ⁶Institut d'Astrophysique Spatiale (CNRS/Univ. Paris-Sud, France), ⁷Freie Universität Berlin (Berlin, Germany).

Summary: Recently developed TES olivine parameters compare well with CRISM and OMEGA olivine detections across the Tyrrhena Terra region. Olivine outcrops along the Libya Montes region are associated with Fe/Mg-smectite, but olivine outcrops across this region south of Libya Montes (Fig. 1) are not well correlated with phyllosilicate outcrops. Altered materials in this region include Fe/Mg-smectite, chlorite, serpentine, carbonate, and maybe zeolite. The occurrence of chlorite, serpentine, and carbonate together likely indicates higher temperature processes occurred. Ongoing work with HiRISE imagery seeks to constrain the occurrences, stratigraphic relations, and relative ages of the smectite and chlorite outcrops.

Introduction: A variety of aqueous alteration materials as well as unaltered mafic rocks have been identified by investigations across the region between Isidis and Hellas [e.g. 1-6]. Exposed views of ancient crustal rocks, lava flows from Syrtis Major, alteration from the Isidis and Hellas impact basins, and multiple stream beds and deltas make this region unique on Mars [e.g. 7-10]. Previous studies of morphologic and spectroscopic features using coordinated CRISM-HRSC and CRISM-HiRISE-CTX imagery observed distinct stratigraphic units containing phyllosilicates, carbonate, olivine and pyroxene in isolated regions [11-12].

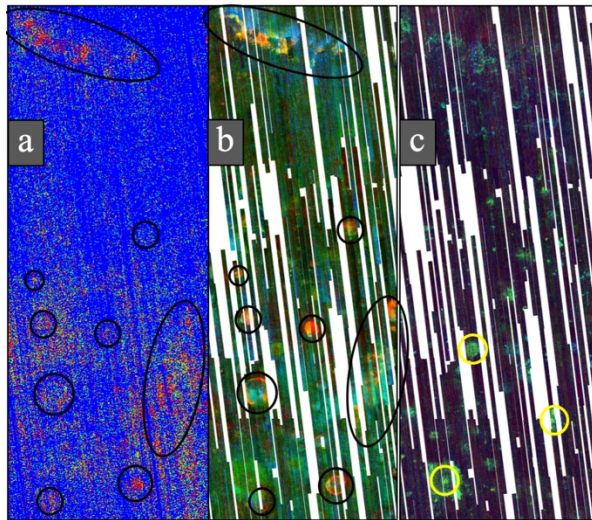


Fig. 1. a) TES map of olivine, b) CRISM multispectral map with olivine in red, c) CRISM multispectral map with Fe/Mg-phyllosilicates in green. The 3 phyllosilicate outcrops ringed in yellow are featured in this study. Each image is ~30 km in width.

Orbital Comparison: We are mapping rock compositions using data from Mars Global Surveyor Thermal Emission Spectrometer (TES), Mars Odyssey Thermal Emission Imaging System (THEMIS) and the Compact Reconnaissance Imaging Spectrometer for Mars (CRISM) multispectral strips. A section of Tyrrhena Terra was analyzed for olivine and Fe/Mg-phyllosilicates (Fig. 1) based on recent studies across Tyrrhena Terra [13-15]. Identification of olivine by TES, THEMIS, and CRISM is consistent for most outcrops, and also confirms and extends previous OMEGA detections [16], although different spectral features are used for these instruments.

Geologic Map: We prepared a geological map of the Tyrrhena Terra region between Libya Montes and Hellas using HRSC nadir image data with the aid of corresponding HRSC DTMs [17]. This map is intended to provide a geological and geomorphological overview of the wider study region. Hence, the mapping scale was selected to be 1:500,000 and the HRSC data were down-sampled to a ground pixel size of 50 m/px for image data and 100 m/px for the DTMs, respectively. Coverage gaps were filled with Viking Orbiter image data (231 m/px) and gridded MOLA topography data (926 m/px). The relative ages of all mapping units were estimated using crater

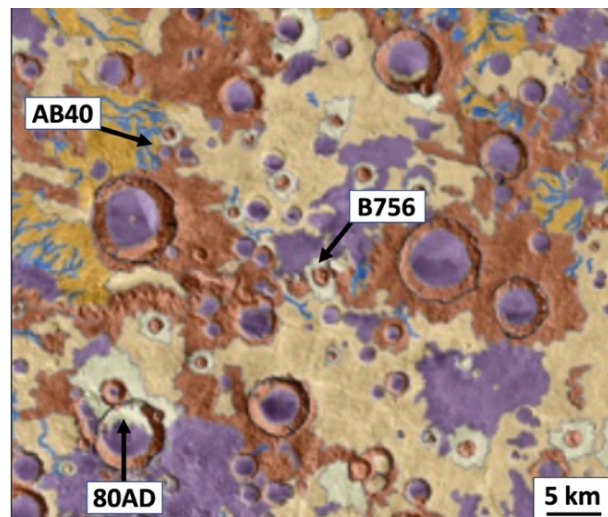


Fig. 2. Subsection of geologic map [17]. The *Noachian massif* (*Nm*) units are mapped in brown, *Noachian/Hesperian heavily eroded materials* (*NHhe*) in orange for fluvially dissected materials (*NHhe1*) and in beige for less degraded materials (*NHhe2*), *Hesperian/Amazonian ridged and smooth plains* (*HARsp*) are mapped in purple, and *Ejecta* is mapped in light green.

size-frequency distributions. Most fluvial channels are incised into Noachian- and Hesperian-aged surfaces. A subset of this geologic map (Fig. 2) displays the region surrounding the phyllosilicate outcrops studied here.

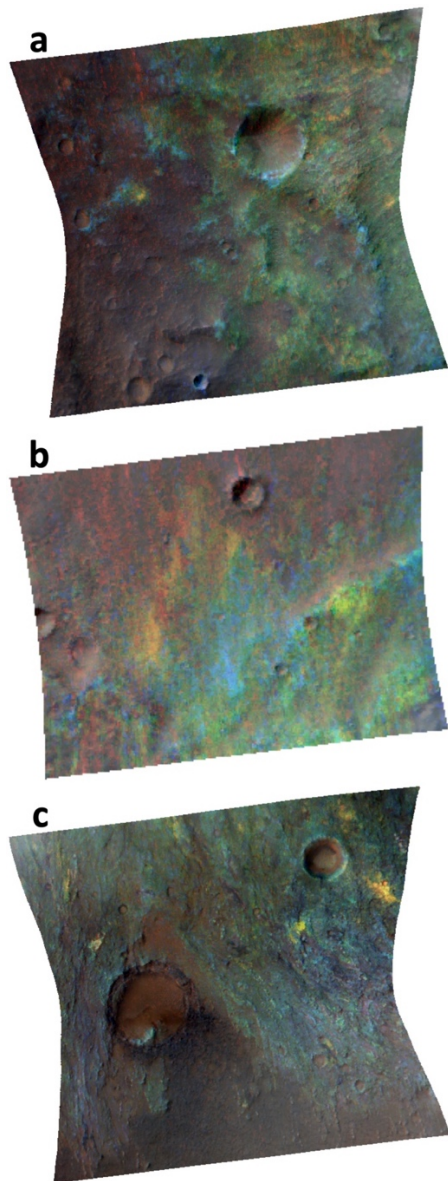


Fig. 3 CRISM views of phyllosilicates from MTRDR projections of PFM (Fe/Mg-phyllosilicates; 45% transparency) over FAL (false color IR) [19], where red/yellow colors indicate chlorites (and Ca/Fe-carbonates), cyan colors indicate Fe-rich smectite, and grey/brown tones represent basaltic materials. a) FRT0000AB40, b) HRS0000B756, c) FRT000080AD.

CRISM Views: We evaluated spectra from 3 targeted CRISM images (Fig. 3) marked on Fig. 2 that capture phyllosilicates in ejecta blankets. We used the MTRDR calibration [18] of these images with parameters PFM (R BD2355, B D2300, G BD2290) and FAL (R R2529, B R1506, G R1080), designed to highlight Fe/Mg-

phyllosilicates and variations in mineralogy across the scene, respectively [19]. Images FRT0000AB40 and HRS0000B756 are associated with fluvial features that have eroded ejecta on the surface, while image FRT000080AD captures ejecta within a crater. Spectra were collected from multiple sites and ratioed to spectrally neutral regions. Selected spectra are shown in Fig. 4 compared to reflectance spectra of minerals. Saponite is found in image FRT0000AB40, sometimes mixed with chlorite and perhaps carbonate, while the spectra of altered outcrops in FRT000080AD are dominated by chlorite, serpentine, carbonate, and maybe zeolite, plus nontronite mixed with the chlorite in some cases. Calcite is most consistent with the carbonate features.

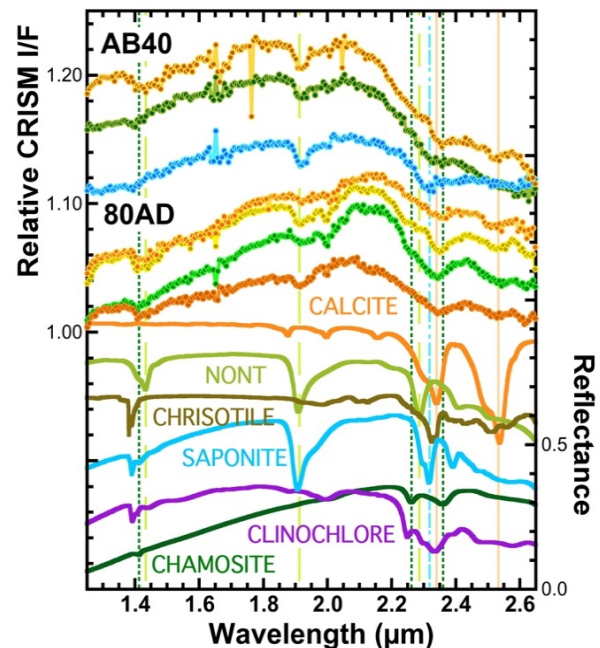


Fig. 4 Selected CRISM spectra of altered outcrops compared with lab spectra of several Fe/Mg- phyllosilicates and calcite.

References: [1] Craddock R. (1994) *LPSC XXV*, 291-292. [2] Ivanov M. & Head J. (2003) *JGR*, 108, E6. [3] Rogers A. & Christensen P. (2007) *JGR*, 112, E01003. [4] Tornabene L. et al. (2008) *JGR*, 113, E10001. [5] Loizeau D. et al. (2012) *Icarus*, 219, 476-497. [6] Rogers A. & Hamilton V. (2015) *JGR*, 120, 62-91. [7] Crumpler L. & Tanaka K. (2003) *JGR*, 108, 12. [8] Jaumann R. et al. (2010) *EPSL*, 294, 272-290. [9] Erkeling G. et al. (2012) *Icarus*, 219, 393-413. [10] Ivanov, M. et al. (2012) *Icarus*, 218, 24-46. [11] Bishop J. et al. (2013) *JGR*, 118, 487-513. [12] Tirsch D. et al. (2018) *Icarus*, 314, 12-34. [13] Lane M. et al. (2019) *9th Mars Conf.*, #6422. [14] Viviano C. & M. Phillips (2019) *9th Mars Conf.*, #6359. [15] Lane M. et al. (2020) *LPSC*, # 2541. [16] Ody A. et al. (2013) *JGR*, 118, 234-262. [17] Tirsch D. et al. (2019) *LPSC*, #1532. [18] Seelos F. et al. (2016) *LPSC*, #1783. [19] Viviano-Beck C. et al. (2014) *JGR*, 119, 2014JE004627.

Acknowledgements: We are grateful for support from MDAF grant # 80NSSC18K1384.